The metal-insulator transition of the Magnéli phase V_4O_7: Implications for V_2O_3

U. Schwingenschlögl, V. Eyert(*) and U. Eckern
Institut für Physik, Universität Augsburg - 86135 Augsburg, Germany

PACS. 71.20.-b – Electron density of states and band structure of crystalline solids.
PACS. 71.27.+a – Strongly correlated electron systems; heavy fermions.
PACS. 71.30.+h – Metal-insulator transitions and other electronic transitions.

Abstract. – The metal-insulator transition (MIT) of the Magnéli phase V_4O_7 is studied by means of electronic-structure calculations using the augmented spherical wave method. The calculations are based on the density-functional theory and the local density approximation. Changes of the electronic structure at the MIT are discussed in relation to the structural transformations occurring simultaneously. The analysis is based on a unified point of view of the crystal structures of all Magnéli phase compounds V_nO_{2n-1} ($3 \leq n \leq 9$) as well as of VO_2 and V_2O_3. This allows to group the electronic bands into states behaving similarly to the dioxide or the sesquioxide. In addition, the relationship between the structural and electronic properties near the MIT of these oxides can be studied on an equal footing. For V_4O_7, a strong influence of metal-metal bonding across octahedral faces is found for states both parallel and perpendicular to the hexagonal $c_{\rm hex}$-axis of V_2O_3. Furthermore, the structural changes at the MIT cause localization of those states, which mediate in-plane metal-metal bonding via octahedral edges. This band narrowing opens the way to an increased influence of electronic correlations, which are regarded as playing a key role for the MIT of V_2O_3.

The vanadium oxides have been attracting a lot of interest for many years, in particular due to their metal-insulator transitions (MIT). Special focus has been on the prototypical compounds VO_2 and V_2O_3, which were studied quite extensively [1–3]. However, much dispute remains as concerns the origin of the phase transitions. While it is agreed that these arise from a delicate interplay of electron-phonon coupling and electronic correlations, the relative importance of these two mechanisms is still under controversal discussion.

At a temperature of 340 K, VO_2 ($3d^1$) undergoes an MIT as well as a simultaneous structural transformation from the rutile to a monoclinic structure. This combined phase transition can be understood from electronic structure calculations, which point to a Peierls instability of the one-dimensional $d_\parallel$ ($d_{x^2-y^2}$) band in an embedding background of the remaining V $3d$ t_{2g} states [4]. Nevertheless, the optical band gap of the insulating phase was missed by the calculations due to the shortcomings of the local density approximation (LDA). However, the interpretation in terms of an embedded Peierls instability was supported by calculations for MoO_2 and NbO_2 [5, 6]. The latter material likewise undergoes an MIT, which is accompanied by structural distortions very similar to those of VO_2. Since within the LDA a finite

(*) E-mail: Volker.Eyert@physik.uni-augsburg.de

optical band gap was obtained for the niobium compound but slightly missed for VO_2, it was concluded that electronic correlations play an albeit small role in the $3d$ system [4, 6].

Stoichiometric V_2O_3 ($3d^2$) shows an MIT at 168 K under ambient pressure, leading from a paramagnetic metallic (PM) to an antiferromagnetic insulating (AFI) phase. Again, there is a simultaneous change of the crystal structure from corundum type to a monoclinic lattice. On doping with small amounts of Al or Cr, V_2O_3 displays a paramagnetic insulating (PI) phase, which still has the corundum structure. However, EXAFS experiments revealed local structural distortions in the PI phase, which are identical to those characterizing the AFI phase but lack long-range order [7]. The phase transitions of V_2O_3 are commonly regarded as being of the Mott- or Mott-Hubbard type, driven by electronic correlations of the V $3d$ states [8]. While LDA calculations for all three phases show only a minor response of the electronic properties to the crystal structure changes occurring at the transitions, LDA + U calculations reproduced the insulating band gap of the AFI phase [9, 10]. In contrast, a correct description of the PM-PI phase transition was achieved only recently by a combination of LDA calculations with the dynamical mean-field theory (DMFT) [11]. In addition, this new approach reproduced the vanadium $S = 1$ state called for by results from polarized X-ray spectroscopy experiments [12].

In order to arrive at a deeper understanding of the MIT of the afore-mentioned vanadium oxides, an identification of the relevant electronic states as well as their response to changes of the crystal structures is highly desirable. In this paper we address this issue by studying the relation between structural and electronic properties in the broader class of the vanadium Magnéli phases. These compounds form a homologous series V_nO_{2n-1} ($3 \leq n \leq 9$) with crystal structures built from characteristic dioxide-like and sesquioxide-like regions. Thus they may be regarded as intermediate between the structures of VO_2 ($n \to \infty$) and V_2O_3 ($n = 2$), allowing for a deeper insight into the crossover from the dioxide to the sesquioxide. Like VO_2 and V_2O_3, all Magnéli phases except for V_7O_{13} show MIT, which are accompanied by structural transformations. Furthermore, they exhibit long-range antiferromagnetic order at Néel temperatures, which, except for VO_2 and V_2O_3, are much lower than the temperatures connected with the MIT [13]. From this it was concluded that the insulating state as well as the MIT are not related to the antiferromagnetic order and, hence, should be studied independently. X-ray refinements suggested that the MIT goes along with charge ordering separating V^{3+} and V^{4+} sites [14]. NMR measurements confirmed this result in general but found the amount of charge disproportionation to be much smaller than one [15]. While our previous study on V_6O_{11} gave strong indications for the predominant influence of electron-lattice interaction in the dioxide-like regions and of electronic correlations in the sesquioxide-like regions of the crystal, respectively [16], the present work concentrates on the sesquioxide-related member V_4O_7 and, hence, allows to draw conclusions about the MIT of V_2O_3.

As the general formula $V_nO_{2n-1} = V_2O_3 + (n-2)VO_2$ suggests, the crystal structures of the Magnéli phases are usually viewed as rutile-type slabs of infinite extension and different thickness, which are separated by shear planes with a corundum-like atomic arrangement [2, 17, 18]. Recently, we have proposed an alternative unified representation of the crystal structures of all Magnéli phases in terms of a regular 3D network of oxygen octahedra, which are partially filled by vanadium atoms [16]. The filled octahedra form chains of length n parallel to the pseudorutile c_{prut} axis, followed by $n-1$ empty sites. While in VO_2 these chains have infinite length, they comprise just two filled octahedra in V_2O_3. The situation is sketched in fig. 1 for V_2O_3 and V_4O_7. Note that only the vanadium atoms are depicted for simplicity. Along the a_{prut}-axis, which is identical to the hexagonal c_{hex}-axis of V_2O_3, vanadium and oxygen layers alternate. In the Magnéli phases, two different types of vanadium layers are distinguished, which likewise alternate along a_{prut}. In V_4O_7 the layers comprise the atoms

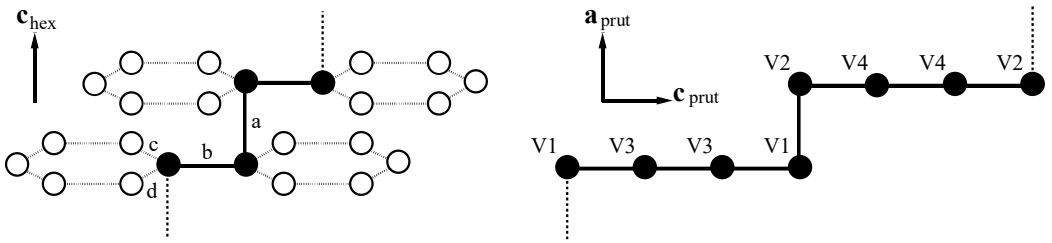

V_2O_3	a	b	c	d
298 K	2.70	2.87	2.87	2.87
125 K	2.75	2.99	2.86	2.88

V_4O_7	V1-V2	V1-V3	V3-V3	V2-V4	V4-V4
298 K	2.77	2.97	2.79	2.93	2.93
120 K	2.78	3.03	2.67	2.83	3.03

Fig. 1 – Building blocks of the crystal structures of V_2O_3 (left side) and V_4O_7 (right side). Only vanadium atoms are shown. The tables list measured V-V distances for both the metallic and the insulating phase.

V1/V3 and V2/V4, respectively. Due to the alternation of the layers and relative shifts of the four-atom chains the end atoms V1 and V2 are found on top of each other, see fig. 1. While neighbouring octahedra share faces along a_{prut} and b_{prut}, metal-metal bonding along all other directions within the layers is via edges (see ref. [4] for further details). As a consequence, the atomic arrangement near the chain ends is V_2O_3-like, whereas the chain centers correspond to the rutile-type regions. By virtue of the just sketched representation of the crystal structures, it is possible to refer the symmetry components of the V $3d$ orbitals of all compounds to a common local coordinate system [4]. In this system the z- and x-axes of the local coordinates are parallel to the apical axis of the local octahedron and the pseudorutile c_{prut}-axis, respectively.

Our LDA calculations are based on the scalar-relativistic augmented spherical wave (ASW) method [19, 20]. Crystallographic data as given by Hodeau and Marezio [21] were used. In order to represent the correct shape of the crystal potential in the large voids of the open crystal structure of V_4O_7, additional augmentation spheres were inserted. Optimal augmentation sphere positions as well as radii of all spheres were automatically generated by the sphere geometry optimization (SGO) algorithm [22]. The basis sets comprised V $4s$, V $4p$, V $3d$, O $2s$, and O $2p$ orbitals as well as states of the additional augmentation spheres. Brillouin zone integrations were performed using an increasing number of $\boldsymbol{k}$ points, ranging from 108 to 2048 points within the irreducible wedge.

Partial V $3d$ densities of states (DOS) resulting from the calculations for the crystal structures of both phases of V_4O_7 are displayed in figs. 2 and 3. In the present paper, we concentrate on the results for the V1/V3 chains. This is motivated by close similarity of the changes in the local surrounding of atom V1 as coming with the structural transformations at the MIT to those known from V_2O_3. According to fig. 1, the V1-V2 and V1-V3 distances both increase at the MIT just as the distances a and b in the sesquioxide at the PM-AFI transition. Since in the latter compound all vanadium atoms are still crystallographically identical, a complete symmetry analysis of the electronic states could not be performed. However, this is possible for V_4O_7. As we have demonstrated in our work on V_6O_{11}, the local atomic arrangements can be directly related to the corresponding electronic properties at these sites [16]. Hence, the V1 site of V_4O_7 is particularly suited to study the influence of the structural changes on the MIT of V_2O_3.

The gross features of the DOS from figs. 2 and 3 are very similar to those known from VO_2 and V_2O_3. As a consequence of the crystal-field splitting of the V $3d$ states due to the surrounding oxygen octahedra, one finds two groups of bands in the energy range displayed. Note that all orbitals are referred to the above-mentioned local coordinate systems [4]. V $3d$

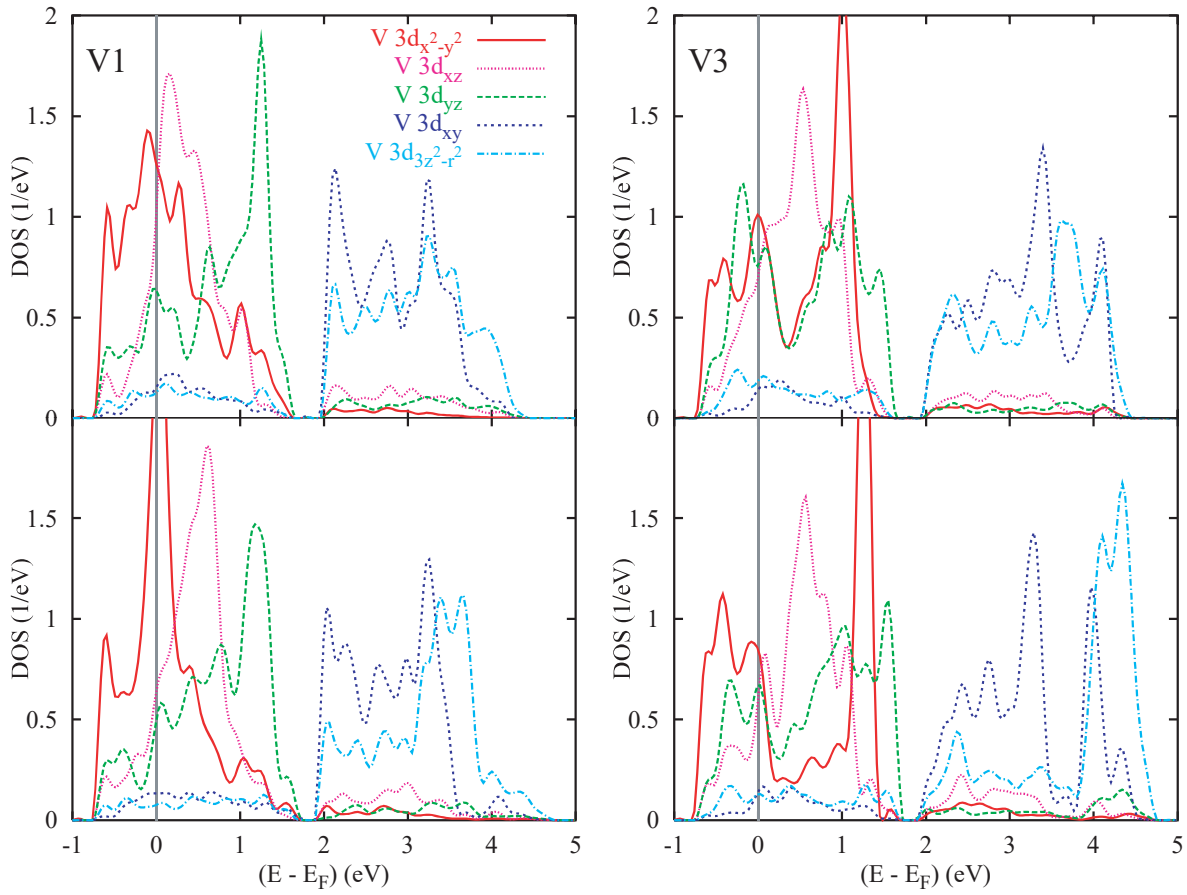

Fig. 2 – Partial V1 and V3 3*d* DOS (per atom) of high- (top) and low-temperature (bottom) V_4O_7.

t_{2g} and e_g states dominate in the energy regions from about -0.6 to 1.8 eV and 2.0 to 4.7 eV, respectively. O 2*p* states, which give larger contributions in the energy region from -8.3 to -3.0 eV, are not included. Oxygen and vanadium contributions in the energy regions where the respective other orbital dominates are less than 10%, but still indicative of covalent bonding. Obviously, the densities of states obtained for the low-temperature phase miss an insulating band gap. As mentioned above, this effect is well known from V_2O_3 and mirrors the shortcomings of the LDA. However, since in the present context we are primarily interested in understanding the relationship between changes of the crystal and the electronic structure at the MIT, these limitations do not prohibit the following considerations. Our low-temperature phase results show a charge disproportionation at the vanadium sites of the order of 0.2 electrons, which is in close agreement with the NMR data [15].

Taking a closer look at the V 3*d* t_{2g} partial DOS we find for the $d_{x^2-y^2}$ DOS a similar behaviour as already observed in VO_2 [4]. Due to strong σ-type metal-metal bonding parallel to the vanadium chains, the chain-center atoms display a distinct splitting of these states. At low temperatures the chains behave differently. Strong V-V dimerization even leads to an enhanced bonding-antibonding splitting of the V3 $d_{x^2-y^2}$ states. In addition, it enforces a sharpening, hence, a stronger localization of the $d_{x^2-y^2}$ states on the V1 atoms, which have only one neighbour along the chains. In contrast, the V4-V4 distance hardly changes, whereas the V2-V4 distance shrinks; this causes an increased bonding-antibonding splitting of the V2 $d_{x^2-y^2}$ states.

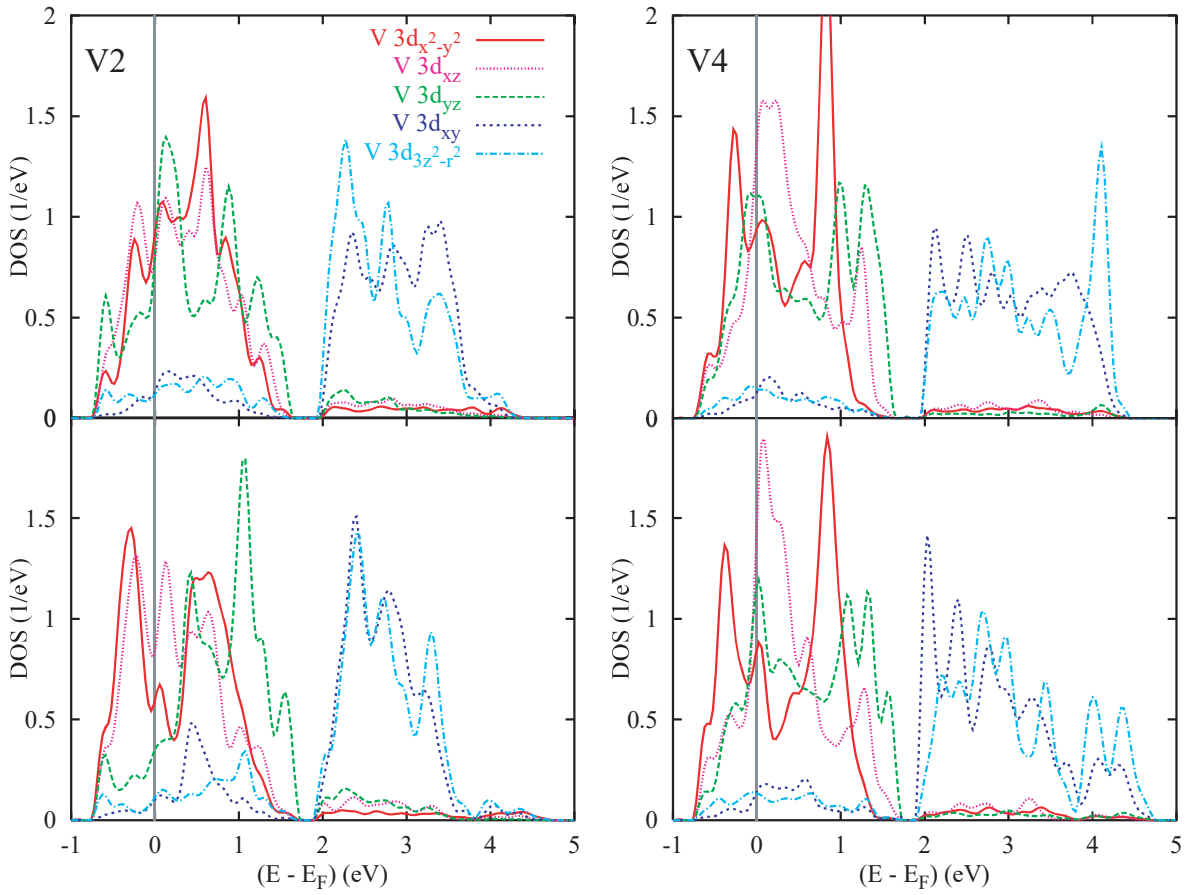

Fig. 3 – Partial V2 and V4 3*d* DOS (per atom) of high- (top) and low-temperature (bottom) V_4O_7.

Changes of the vanadium d_{xz} partial DOS at the transition are less significant and consist mainly of an energetical up- and downshift of these states as observed for atom V1 and V2, respectively. These shifts are due to increased and decreased lateral (perpendicular to c_{prut}) vanadium atom displacements away from the centers of gravity of the surrounding oxygen octahedra and, hence, derive from the changes of the V 3*d*-O 2*p* overlap. They are thus well understood in terms of the antiferroelectric zigzag-like displacement already observed for vanadium dioxide [4]. However, note that in the latter compound finite lateral displacements occur only in the low-temperature phase, whereas V_4O_7 displays them in both phases. Interestingly, the lateral displacement is much larger for the chain-end atoms as compared to atoms V3 and V4. This is due to a slight rotation of the chains away from the pseudorutile axis c_{prut}, which has been observed for all Magnéli phases [16]. In passing, we mention that metal-metal overlap is less important for the d_{xz} orbitals.

The situation is more complicated for the V d_{yz} orbitals, which are strongly influenced by different kinds of hybridizations. In VO_2, these orbitals take part in metal-metal overlap across octahedral faces along both a_{rut} and b_{rut} [4]. In addition, the antiferroelectric displacement of the vanadium atoms leads to increased *d*-*p* overlap causing an upshift of the antibonding, *d*-dominated states. In V_4O_7, the atoms V3 and V4 display neither considerable antiferroelectric displacements nor metal-metal overlap along a_{prut}, since there are no vanadium neighbours along this direction. As a consequence, the pronounced double-peak structure of the V3 and V4 d_{yz} partial DOS is indicative of bonding-antibonding splitting due to V1-V3 and V2-V4 overlap, respectively, across the shared octahedral faces parallel

to b_{prut}. The chain-end atoms, in contrast, apart from participating in the V1-V3 and V2-V4 overlap parallel to b_{prut}, take part in V1-V2 bonding along a_{prut}. The d_{yz} partial DOS of atoms V1 and V2 thus display features reminiscent of the corresponding partial DOS of atoms V2/V3 and V1/V4, respectively. In particular, we observe the close resemblance of the d_{yz} partial DOS of these two atoms in the low-temperature phase. Being subject to two different types of overlap, the d_{yz} orbitals of V1 and V2 undergo two intertwining bonding-antibonding splittings leading to the complicated triangular-like shape of the corresponding partial DOS similar to that known from the V $3d$ a_{1g} states of V_2O_3 [11]. In addition, their form is affected by the above-mentioned zigzag-like displacement of the chain-end atoms causing increased metal-oxygen overlap at these sites. As a consequence, the centers of gravity of the V1 and V2 d_{yz} partial DOS are shifted to higher energies. Finally, the changes of the V2 d_{yz} partial DOS, in particular the closer resemblance of this DOS to the respective curve of atom V1 in the low-temperature phase, can be traced back to the reduced relative displacement of these atoms parallel to c_{prut}. This causes an improved alignment of the V1-V2 bond parallel to a_{prut} and, hence, an increased overlap along this latter direction.

To summarize our results, we find the electronic properties of V_4O_7 to be strongly influenced by the local environment of each atom. While, in general, the overlap of O $2p$ and V $3d$ states places the V $3d$ t_{2g} states near the Fermi energy, the detailed electronic structure of the latter are subject to the local metal-metal coordination. In particular, we have found a strong bonding-antibonding splitting of the $d_{x^2-y^2}$ states of the chain-center atoms and, in the low-temperature structure, also for atom V2. This is in close analogy to the behaviour of these states in VO_2, where it is likewise enforced by metal-metal dimerization. In contrast, the V1 $d_{x^2-y^2}$ states display a distinct sharpening since they do not take part in V-V dimerizations along the chains. Hence, they are more susceptible to electronic correlations. A similar behaviour should be observed for V_2O_3, where the corresponding distance (labelled b in fig. 1) likewise increases.

For the d_{xz} and d_{yz} states we observe a distinct response to the displacement of the vanadium atoms perpendicular to c_{prut} relative to the centers of their respective octahedra, leading to energetical up- and downshift of these states. However, the d_{yz} partial DOS of all atoms are mainly affected by the metal-metal bonding across the shared octahedral faces. As a consequence, they show bonding-antibonding splitting as seen in the d_{yz} partial DOS of the chain-center atoms, which are subject to bonding only parallel to b_{prut}. The situation is more complicated for atoms V1 and V2, which take part in the just mentioned V1-V3 and V2-V4 bonding parallel to b_{prut} as well as in V1-V2 bonding along a_{prut}. They end up with a d_{yz} partial DOS similar to that of the a_{1g} states of V_2O_3. Note that the latter states mediate metal-metal bonding parallel to a_{prut} ($\hat{=} c_{\mathrm{hex}}$).

In conclusion, similar to the situation in other Magnéli phases [16], the electronic structure of V_4O_7 arises as a mixture of features characteristic of either the dioxide or the sesquioxide. Note that the local environment of the chain-end atom V1 bears a close resemblance to the situation in V_2O_3. In both compounds this atom shows an increasing separation from its vanadium neighbours at the transition. From our results for V_4O_7 we are thus able to draw the following conclusions for the sesquioxide: First, while the metal-metal bonding across the octahedral faces parallel to a_{prut} seems to have the largest effect on the d_{yz}, hence, the a_{1g} states of V_2O_3, d-d hybridization across the faces parallel to b_{prut} is rather large. Instead, it causes strong splitting of the electronic states. Second, due to the reduced metal-metal bonding across the octahedral edges parallel to c_{prut} the V $d_{x^2-y^2}$ states should undergo increased localization at the transition also in V_2O_3. This conclusion supports previous work by Dernier, who concluded from a comparison of pure and doped V_2O_3 as well as Cr_2O_3 that the metallic properties are intimately connected with the V-V hybridization across the shared

octahedral edges rather than with hopping processes within the vanadium pairs along the hexagonal c-axis [23]. From this point of view, the MIT thus arises from the crystal structure changes occurring at the transition. Via strong electron-phonon coupling these distortions translate into a narrowing of the bands perpendicular to c_{hex} and, eventually, allow for an increased influence of electronic correlations in the insulating phase. From the presence of local octahedral distortions in the PI phase as reported by Pfalzer *et al.* [7], we expect this scenario to hold for both the PM-AFI and the PM-PI phase transition.

* * *

Fruitful discussions with S. Horn, S. Klimm and P. Pfalzer are gratefully acknowledged. This work was supported by the Deutsche Forschungsgemeinschaft through SFB 484.

REFERENCES

[1] Goodenough J. B., *Prog. Solid State Chem.*, **5** (1971) 145.
[2] Brückner W., Oppermann H., Reichelt W., Terukow J. I., Tschudnowski F. A. and Wolf E., *Vanadiumoxide* (Akademie-Verlag, Berlin) 1983.
[3] Imada M., Fujimori A. and Tokura Y., *Rev. Mod. Phys.*, **70** (1998) 1039.
[4] Eyert V., *Ann. Phys. (Leipzig)*, **11** (2002) 650.
[5] Eyert V., Horny R., Höck K.-H. and Horn S., *J. Phys. Condens. Matter*, **12** (2000) 4923.
[6] Eyert V., *Europhys. Lett.*, **58** (2002) 851.
[7] Pfalzer P., Will J., Nateprov A., Klemm M., Eyert V., Horn S., Frenkel A. I., Calvin S. and denBoer M. L., *Phys. Rev. B*, **66** (2002) 085119.
[8] Castellani C., Natoli C. R. and Ranninger J., *Phys. Rev. B*, **18** (1978) 4945; 4967; 5001.
[9] Mattheiss L. F., *J. Phys. Condens. Matter*, **6** (1994) 6477.
[10] Ezhov S. Yu., Anisimov V. I., Khomskii D. I. and Sawatzky G. A., *Phys. Rev. Lett.*, **83** (1999) 4136.
[11] Held K., Keller G., Eyert V., Vollhardt D. and Anisimov V. I., *Phys. Rev. Lett.*, **86** (2001) 5345.
[12] Park J.-H., Tjeng L. H., Tanaka A., Allen J. W., Chen C. T., Metcalf P., Honig J. M., de Groot F. M. F. and Sawatzky G. A., *Phys. Rev. B*, **61** (2000) 11506.
[13] Kachi S., Kosuge K. and Okinaka H., *J. Solid State Chem.*, **6** (1973) 258.
[14] Marezio M., McWhan D. B., Dernier P. D. and Remeika J. P., *Phys. Rev. Lett.*, **28** (1972) 1390.
[15] Gossard A. C., Remeika J. P., Rice T. M., Yasuoka H., Kosuge K. and Kachi S., *Phys. Rev. B*, **9** (1974) 1230.
[16] Schwingenschlögl U., Eyert V. and Eckern U., *Europhys. Lett.*, **61** (2003) 361.
[17] Magnéli A., *Acta Chem. Scand.*, **2** (1948) 501.
[18] Andersson S. and Jahnberg L., *Ark. Kemi*, **21** (1963) 413.
[19] Williams A. R., Kübler J. and Gelatt C. D. jr., *Phys. Rev. B*, **19** (1979) 6094.
[20] Eyert V., *Int. J. Quantum Chem.*, **77** (2000) 1007.
[21] Hodeau J.-L. and Marezio M., *J. Solid State Chem.*, **23** (1978) 253.
[22] Eyert V. and Höck K.-H., *Phys. Rev. B*, **57** (1998) 12727.
[23] Dernier P. D., *J. Phys. Chem. Solids*, **31** (1970) 2569.